

Spontaneous breaking of chiral symmetry in achiral bent-core liquid crystals: Excluded volume effect

Dipak Patra and Arun Roy*

Soft Condensed Matter Group, Raman Research Institute, Bangalore 560080, India

(Received 18 January 2023; accepted 14 March 2023; published 24 March 2023)

Bent-Core banana-shaped molecules exhibit tilted polar smectic phases with macroscopically chiral layer order even though the constituent molecules are achiral in nature. Here, we show that the excluded volume interactions between the bent-core molecules account for this spontaneous breaking of chiral symmetry in the layer. We have numerically computed excluded volume between two rigid bent-core molecules in a layer using two types of model structures of them and explored the different possible symmetries of the layer that are favored by the excluded volume effect. For both model structures of the molecule, the C_2 symmetric layer structure is favored for most values of tilt and bending angle. However, the C_s and C_1 point symmetries of the layer are also possible for one of the model structures of the molecules. We have also developed a coupled XY -Ising model and performed Monte Carlo simulation to explain the statistical origin of spontaneous chiral symmetry breaking in this system. The coupled XY -Ising model accounts for the experimentally observed phase transitions as a function of temperature and electric field.

DOI: [10.1103/PhysRevE.107.034704](https://doi.org/10.1103/PhysRevE.107.034704)

I. INTRODUCTION

Chirality is associated with many natural phenomena occurring in microscopic as well as in macroscopic systems. According to Lord Kelvin, an object is *chiral* when it is not superimposable with its mirror image. Chirality is manifested in various liquid crystalline phases such as cholesteric phase, blue phases, chiral smectic phases, twist-bend nematic phases, etc. [1,2]. In general, a macroscopic phase shows chirality when its constituent molecules are chiral. But, achiral molecules can sometimes exhibit macroscopic chiral phases leading to spontaneous breaking of chiral symmetry. The bent-core (BC) banana-shaped molecules are now known to exhibit such chiral symmetry breaking in some of their liquid crystalline phases [3–5]. The underlying microscopic molecular mechanism responsible for this chiral symmetry breaking is still not well understood.

The BC molecule consists of two rigid rodlike arms joined end to end at an angle of about 120 degrees between them. In addition, flexible aliphatic chains are usually attached at both the free ends of the molecule. The line joining the ends of the molecule is defined as the long axis. Because of the bent shape of the molecule, it has a transverse shape polarity giving rise to the C_{2v} point symmetry and the BC banana-shaped molecules are *achiral* in nature. In their tilted polar smectic phases, the BC molecules arrange themselves in fluid layers and their long axes on average tilted with respect to the layer normal in a given layer as shown in Fig. 1. The average orientation direction of the long axis \hat{l} of the molecules in a layer is denoted by the apolar unit vector \hat{n} known as the director. In

addition, the transverse bending direction \hat{p} of the molecules also align on average giving the polar order \vec{P} in the layer. The chirality of a layer arises depending on the mutual orientations of three directions namely the layer normal (\hat{k}), the director (\hat{n}), and the polar order (\vec{P}). The chirality of a layer can be defined in terms of the sign of the vector triple product $(\hat{k} \cdot \hat{n})[(\hat{k} \times \hat{n}) \cdot \vec{P}]$ consistent with the apolar nature of both the director and the layer normal. The chirality of a layer can then be quantified by $\cos \psi = \hat{P} \cdot (\hat{k} \times \hat{n}) / \sin \theta$, where θ and ψ are the tilt angle and roll angle of the molecules in the layer, respectively. The roll angle ψ defines the rotation of the tilted BC molecule about its long axis. When the roll angle ψ is equal to 0 or π , the polar axis \hat{P} , projection of \hat{n} on the layer plane and layer normal are mutually orthogonal describing a right or left handed coordinate system, respectively. There is only a twofold rotation axis parallel to the polar axis \hat{P} with no mirror plane symmetry giving rise to the chiral C_2 point symmetry of a layer. When ψ is equal to $\pi/2$ or $3\pi/2$, the unit vectors \hat{P} , \hat{n} , and \hat{k} all lie in the same plane which itself becomes a mirror plane symmetry of the layer. So, the layer has an achiral C_s point symmetry. For intermediate values of ψ , the layer has the lowest C_1 point symmetry giving rise to the most general chiral tilted polar smectic ($SmCPG$) order in a layer.

The most commonly observed tilted polar smectic ($SmCP$) phase of these BC molecules is the B_2 phase [3,6–10]. In the B_2 phase, the roll angle ψ is equal to 0 or π and the layer is chiral with C_2 symmetry. The stacking of these chiral $SmCP$ layers with synclitic or anticlitic tilt order and ferro or antiferro polar order between successive layers has been observed in the B_2 phase. Depending on the relative orientations of tilt and polar directions in successive layers, there are four possible configurations of B_2 phase with same free energy and all of them generally found to coexist in this phase. Recently,

*aroy@rri.res.in

some colloidal systems have also been found to exhibit these kind of phases [11].

The possibility of most general smectic (SmCG) phase with C_i point symmetric of the layers was first predicted by de Gennes in the first edition of his classic book [1]. Brand *et al.* theoretically discussed properties and applications of the general SmCPG phase [12]. The experimental evidence of the existence of this general SmCPG phase has also been reported [13–18]. Assuming a simple triangular shape of the BC molecules, Bailey *et al.* calculated the excluded volume between the molecules and predicted undulated layer structure with local C_1 symmetry [19]. The smectic phase denoted as SmTP phase with C_s point symmetry of the layers has been reported experimentally [20,21], where T denotes the ‘Tipping’ angle analogous to the ‘Leaning’ angle of the BC molecules in the layer.

To better understand the complex phase behavior of BC molecules, a large number of studies using phenomenological theory, molecular theory, molecular dynamics, and Monte Carlo (MC) simulations have been performed [11,22–28]. But few of these studies addressed or resolved the microscopic origin of chiral symmetry breaking in the layer. Roy *et al.* has shown using a phenomenological theory that BC molecules can exhibit layer structure with C_2 , C_1 , and C_s point symmetries depending upon phenomenological constants and discussed the stability of polar smectic A (SmAP) phase using uniaxial nematic interaction between the rodlike arms of the BC molecules [22]. But they did not consider the molecular interactions which could lead to tilted polar smectic phases. Xu *et al.* addressed the excluded volume effect as the possible reason for the origin of chiral behavior in the bent-core molecular systems using Monte Carlo simulation [24]. In their simulation, a BC molecule was made of seven spherical beads and the soft repulsive Weeks-Chandler-Andersen (WCA) interaction potential between two spherical beads of different molecules was used. They did not observe any tilted polar smectic phase but found chiral crystal phases. So, the role of excluded volume effect in the chiral symmetry breaking of a tilted polar smectic layer was not clear. Lansac *et al.* considered the BC molecule consisting of two connected spherocylinders and performed MC simulation taking hard body interaction between two BC molecules. But, they did not find any tilted smectic phase. Emelyanenko *et al.* have shown the stability of SmCP layer by considering steric, dispersion and dipole-dipole interactions between two molecules made of interconnected rigid rods [28]. They did not find C_1 symmetric SmCPG chiral layer. Yang *et al.* have shown the stability of SmCP phase using Brownian dynamics simulation. The molecular model and interaction potential employed in their simulation are similar to Xu *et al.* [24]. So, it is clear that the molecular origin of the spontaneous breaking of chiral symmetry has not been resolved.

We consider here the role of hard body interaction or excluded volume effects on the chiral symmetry breaking in a layer of the tilted polar smectic phase of BC molecules. We directly compute the excluded volume between two BC molecules in a tilted smectic layer and our approach is different from previous molecular dynamics and Monte Carlo simulation studies. It is well known that the excluded volume effect plays an important role in phase ordering and properties

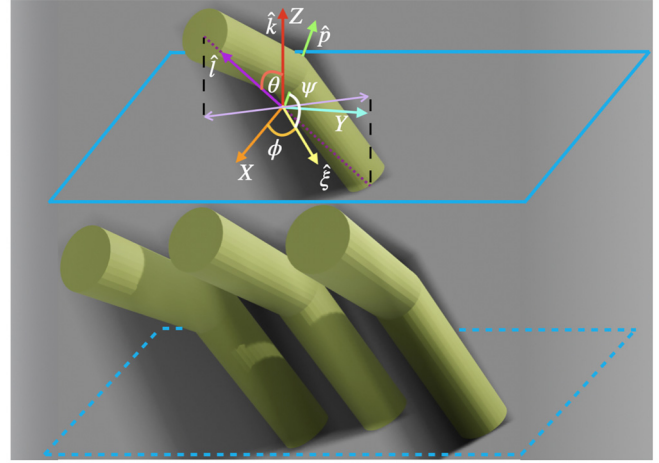


FIG. 1. Schematic representation of the orientation of a BC molecule in a perfectly ordered tilted polar smectic layer where θ , ϕ and ψ are the Euler angles. The layer normal \hat{k} is parallel to z axis and the XY plane is the layer plane. The double-headed arrow represents the projection of the long axis on the layer plane. For a perfectly ordered layer, the director \hat{n} and polar order \hat{P} are parallel to \hat{l} and \hat{p} of the molecules, respectively. The unit vector $\hat{\xi} = (\hat{k} \cdot \hat{l})(\hat{k} \times \hat{l}) / |(\hat{k} \cdot \hat{l})(\hat{k} \times \hat{l})|$ represents the tilt direction of a molecule which is perpendicular to the (\hat{l}, \hat{k}) plane.

of soft matter systems such as van der Waals correction to Ideal gas law, Onsager’s theory of nematic to isotropic transition [29]. Two types of models for the BC molecules are considered in our numerical calculation of excluded volume between two molecules in a layer. We show that the excluded volume effect favours the chiral symmetry breaking in the SmCP layer of BC molecules. We have also constructed a coupled XY -Ising model to describe the statistical origin of chiral symmetry breaking. Monte Carlo simulation studies using our XY -Ising model were performed to find the possible phases with temperature as well as under applied electric field.

II. MODEL

For the computation of the excluded volume, we have considered two types of structural models for the BC molecules. In one model, hard spherical beads are joined together to form the BC molecule as shown in Fig. 2(a). The molecular parameters in this model are bending angle β , radius of the spherical beads R , and the total number of beads N . In the other model, the BC molecule consists of two spherocylindrical arms of radius R and length $(N - 1)R$ joined end to end with an angle β between their long axes as shown in Fig. 2(b).

The analytical calculation of excluded volume even for simple rodlike molecules is a formidable task. Onsager first derived an approximate analytical expression for the excluded volume between hard spherocylindrical rods in the limit of large length to diameter ratio of the rods. Based on these results, he accounted for the isotropic to nematic transition for this hard rod system at sufficiently high concentrations [29]. We have used numerical tools to compute the excluded volume of bent-core molecules in a layer of their tilted polar smectic phase. To reduce the complexity of the problem, we

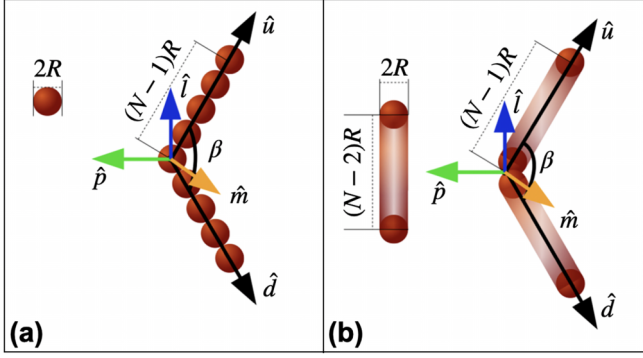


FIG. 2. The model structures (a) bead model (b) hard spherocylinder (HSC) model of a BC molecule used in the computation of excluded volume. The unit vectors \hat{l} , \hat{p} , and \hat{m} are body fixed axes. The unit vectors \hat{u} and \hat{d} represent the orientation of upper and lower arms, respectively.

assume that all molecules in a layer have their centers in the plane of the layer and also they have the same orientation. A molecular frame $(\hat{l}, \hat{p}, \hat{m})$ as shown in Fig. 2 can be used to specify the orientation of a BC molecule in a layer. Then the orientation of a BC molecule with respect to the layer frame coordinate system is represented by the Euler angles (tilt angle θ , azimuthal angle ϕ , roll angle ψ) [30] as shown in Fig. 1.

We compute the excluded volume between the molecules by finding the closest approach of a molecule around a fixed molecule in a layer. Consider two BC molecules with the bead type structure which are initially juxtaposed with each other in a layer with a given orientation. Now keeping one of the molecules fixed, the other molecule is moved on the layer plane in a particular direction with an azimuthal angle α without changing its orientation. At each position of the second molecule, the distance between each bead of one molecule is calculated with respect to the beads of the other molecule. The second molecule is moved in that direction until the minimum of these interbead distances exceeds $2R$. This position \vec{r}_α gives the vectorial distance of the closest approach of the second molecule with respect to the first molecule in that direction α . At this position, the coordinates of all the beads of the second molecule are stored for this particular value of α . Then by repeating the above procedure by varying α from 0 to 2π , a three-dimensional excluded volume region around the fixed molecule can be constructed. This excluded volume region consists of two parts divided by the midplane of the layer.

The infinitesimal excluded area between the direction α and $\alpha + \delta\alpha$ is given by $\delta\vec{A}_{\text{ex}} = \frac{1}{2}\vec{r}_\alpha \times \vec{r}_{\alpha+\delta\alpha}$. The area vector direction is parallel to the layer normal or z axis. Then the infinitesimal excluded volume of the upper half part between α and $\alpha + \delta\alpha$ is $\frac{N-1}{2}R(\hat{u} \cdot \vec{r}_\alpha \times \vec{r}_{\alpha+\delta\alpha})$, where the unit vector \hat{u} denotes the orientation of the upper arms of the BC molecules in the layer. Similarly, the infinitesimal excluded volume of the lower half part is given by $\frac{N-1}{2}R(-\hat{d} \cdot \vec{r}_\alpha \times \vec{r}_{\alpha+\delta\alpha})$, where the unit vector \hat{d} denotes the orientation of the lower arms of the BC molecules in the layer. So, the total infinitesimal excluded volume between the direction α and $\alpha + \delta\alpha$ is $\delta V_{\text{ex}} = \frac{N-1}{2}R(\hat{u} - \hat{d}) \cdot (\vec{r}_\alpha \times \vec{r}_{\alpha+\delta\alpha})$. The total excluded volume V_{ex} is obtained by integrating δV_{ex} over the angle α from 0 to 2π .

We numerically compute the excluded volume by discretizing α between 0 to 2π into M small intervals. Then summing over these discrete values of α , the total excluded volume can be written as

$$V_{\text{ex}} = 2(N-1)RA_{\text{ex}} \sin \frac{\beta}{2} \cos \theta,$$

where the magnitude of the total excluded area is given by

$$A_{\text{ex}} = \frac{1}{2} \sum_{i=1}^M |\vec{r}_i \times \vec{r}_{i+1}|$$

and \vec{r}_i is the closest approach of the second molecule in the α_i -th direction. A dimensionless form of the excluded volume can be obtained by dividing the computed excluded volume by the volume $4\pi R^3/3$. Henceforth, this dimensionless excluded volume is denoted as V_{ex} in the rest of the article. The results presented in this article have been computed using $N = 9$. For other values of N , the excluded volume just scales with N without changing the conclusions.

Similarly, the excluded volume between two BC molecules with spherocylindrical arms can be calculated. The algorithms as discussed in the articles [31,32] for finding the shortest distance between two straight rods are utilised to find the closest approach between two molecules. The consistency of our algorithm was checked by computing the excluded volume for $\beta = \pi$ which can be calculated analytically.

We have also computed the excluded volume for nontilted molecules in the layer with $\theta = 0$. In this case, the azimuthal angle ϕ can be chosen arbitrarily as $\phi = 0$. We calculate the excluded volume between two molecules for different relative orientations of their polar directions \hat{p} . From the symmetry of the problem, the excluded volume depends only on the difference in the azimuthal angles $\delta\psi$ between the polar directions. Without any loss of generality, we fixed $\psi = 0$ for the first molecule and computed the excluded volume for different values of ψ of the second molecule between 0 to 2π using the algorithm discussed above.

The excluded volume between the molecules makes a purely entropic contribution to the free energy. The free energy density is proportional to the excluded volume as can be shown analytically for a dilute hard sphere system. So, the molecular configuration associated with the minimum V_{ex} is favored energetically.

III. RESULTS AND DISCUSSIONS

In the SmA and SmAP phase, the long axes of the BC molecules are on average parallel to the layer normal. In the SmA phase, the layers do not possess any polarization whereas in the SmAP phase, the layers have an in-plane polar order. The excluded volume of two such nontilted BC molecules in a smectic layer is computed for various relative orientations $\delta\psi$ between their bending directions as shown in Fig. 3. Excluded volume is minimum for $\delta\psi = 0^\circ$ or 360° and shows a symmetric maximum at 180° as expected from the packing considerations. The excluded volume interaction therefore tends to align the bending directions of the BC banana-shaped molecules in the nontilted smectic layers giving rise to the polar SmAP order. This result is similar to that found assuming dispersion interaction between the BC molecules [28]. The

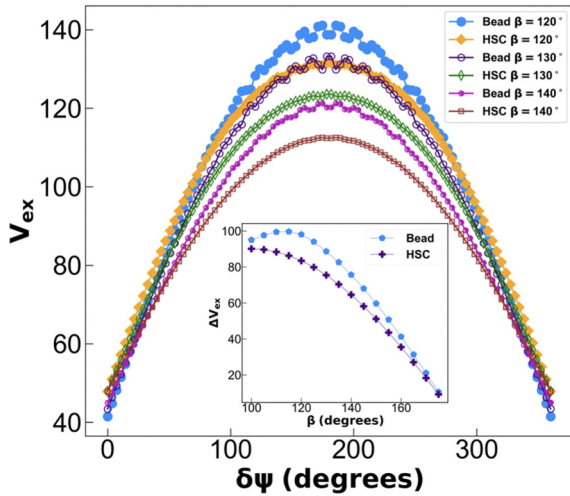


FIG. 3. The variation of the excluded volume V_{ex} with the relative azimuthal angle $\delta\psi$ between two molecules for an orthogonal smectic layer. Inset shows the difference in V_{ex} corresponding to $\delta\psi = \pi$ and 0 for different values of β .

inset of Fig. 3 depicts the variation of the excluded volume difference between the parallel and antiparallel configuration of the bending direction of the molecules as a function of the bending angle β . This excluded volume difference ΔV_{ex} can be associated with the free energy barrier between the parallel and antiparallel configuration of the bending direction of the molecules. Hence, it contributes to the stability of the SmA or SmAP phases. For nearly rodlike molecules with $\beta \sim 180^\circ$, the barrier height is quite low stabilising the SmA phase as expected. These results agree with the observation of SmAP and SmA phases for lower and higher bending angles, respectively, in the MC simulation of HSC model of the BC molecules [26]. The ΔV_{ex} is always higher for the bead model favoring the SmAP phase compared to the HSC model of the BC molecules.

In the tilted polar smectic phase, the long axes of the BC molecules in a layer are tilted with respect to the layer normal. The excluded volume between the molecules in a layer depends on the tilt angle θ , roll angle ψ , and bending angle β of the molecules. The excluded volume as a function of ψ varies with a periodicity of π and is symmetric about $\pi/2$ as expected from the symmetry of the system. Figure 4 shows the variation of excluded volume with ψ for different fixed values of θ and β assuming the HSC model structure of the BC molecules. The excluded volume is minimum at $\psi = 0$ and π indicating that it favours chiral symmetry breaking with the C_2 point symmetry of the layer. The profile of the excluded volume as a function of ψ remains qualitatively same for different values of θ and β . However, for bead model of the BC molecule, the variation of excluded volume with ψ strongly depends on θ and β of the molecules as shown in Fig. 5. The profile of excluded volume with ψ can be classified into four types based on the position of extrema at different values of ψ . In the first type, the excluded volume remains almost constant for different values of ψ as shown in plot I. Hence, the layers with C_1 , C_2 , and C_s symmetries have the same excluded volume and are equally probable. This behavior occurs

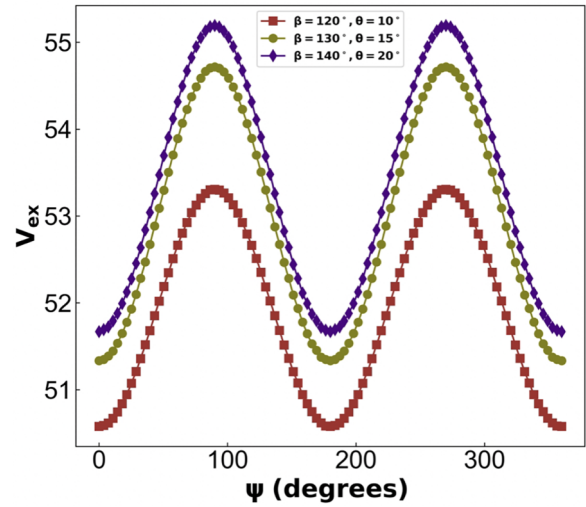


FIG. 4. The variation of excluded volume V_{ex} as a function of roll angle ψ for the HSC model.

for high and low values of β and θ of the BC molecules, respectively. In the second case (plot II), the excluded volume has degenerate minima for a range of values of ψ about zero in addition to the maximum at $\psi = 90^\circ$. The degenerate minima of the excluded volume favour both C_1 and C_2 symmetric layer structures with chiral symmetry breaking. This behavior was found only for $\beta > 120^\circ$ and moderate values of θ . In the third case (plot III), the excluded volume is minimum only at $\psi = 0$ favoring the C_2 symmetric SmCP layer structure with

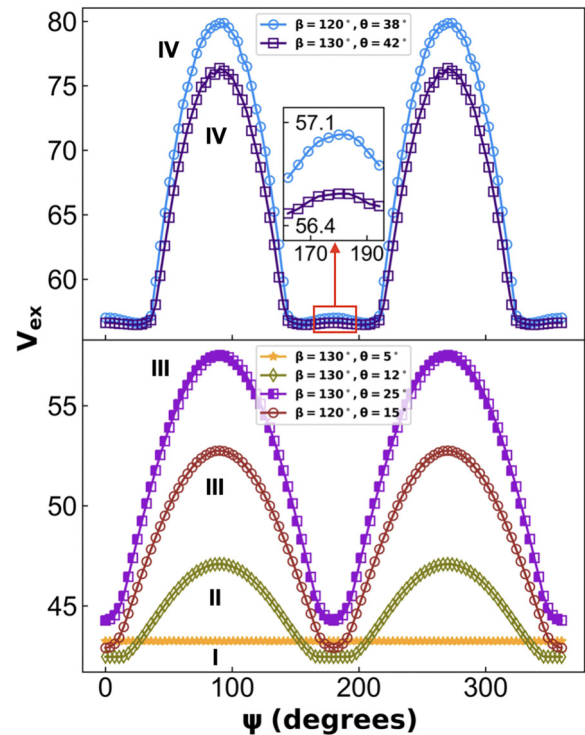


FIG. 5. The variation of V_{ex} as a function of roll angle ψ for the bead model. Inset shows the magnified view of the indicated region demonstrating the maximum at $\psi = 180^\circ$ for higher values of θ .

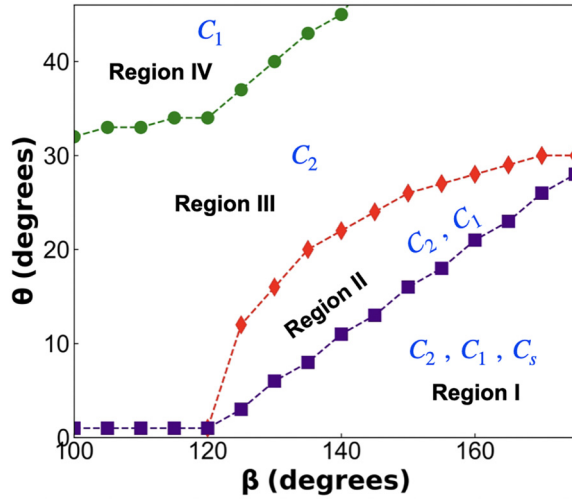


FIG. 6. The stability diagram in the θ - β plane representing the regions of stability of the different symmetries of the layers obtained from the excluded volume interactions for bead model of the molecules.

spontaneous breaking of chiral symmetry. For the fourth type, the excluded volume has a minimum only at an intermediate value of ψ between 0 and $\pi/2$ as shown in plot IV. It should be noted that the excluded volume is maximum at $\psi = 0$ and π in this case as shown in the inset of Fig. 5. Hence, the most general SmCPG layer structure with C_1 point symmetry is favoured. This case was found for large θ and values of β near 120° of the molecules. Based on these excluded volume analyses, a stability diagram in the θ - β parameter plane for the different possible symmetries of the layer is constructed as shown in Fig. 6. The figure displays four separate regions corresponding to different possible symmetries of the layer. In region I, the C_1 , C_2 , and C_s symmetries of the layers are possible due to excluded volume interaction. In region II, C_1 and C_2 symmetries are favored. In regions III and IV, only the C_2 and C_1 symmetries of the layer are found, respectively. The layers can have C_s symmetry only in the region I with high values of bending angle and low values of tilt angle. Whereas, the layers with C_1 symmetry are possible in regions I, II, and IV. However, the C_2 symmetric layer structure can be found for most values of β and θ studied in our model as shown in Fig. 6.

Therefore the excluded volume interaction for both HSC and bead models of the BC molecules predicts C_2 symmetric layer structure with chiral symmetry breaking as found in the B_2 phase experimentally. Depending on the tilt and bending angle, the bead model also predicts the possibility of the existence of the C_1 and C_s symmetric layer structures. As the excluded volume has equal minima both at $\psi = 0$ and π , the right and left handed structures are equally probable. This equality arises due to the achiral nature of the BC molecules.

The variation of excluded volume with tilt angle θ for both HSC and bead model of the BC molecules is presented in Fig. 7 for a fixed value of $\psi = 0^\circ$ and for different values of β . The excluded volume increases monotonically with θ for all values of β for the HSC model as shown in Fig. 7(a).

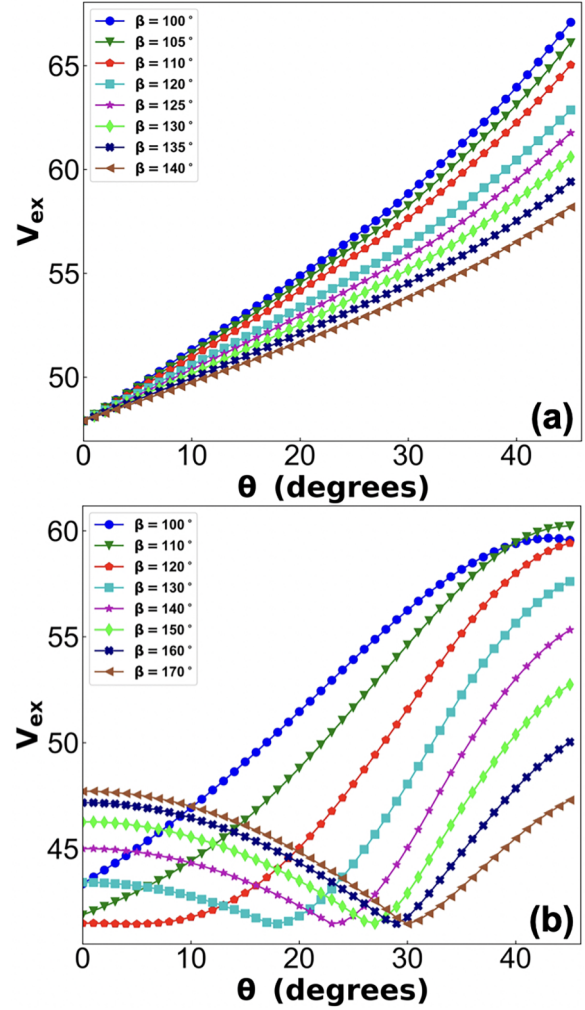


FIG. 7. The variation of V_{ex} with tilt angle θ at $\psi = 0$ or π for (a) HSC model and (b) bead model of the molecules.

Hence, the excluded volume for SmAP layer corresponding to $\theta = 0^\circ$ is always lower than that for the tilted polar smectic layer with $\theta \neq 0^\circ$. Therefore, the SmAP phase is favored compared to the SmCP phase for the HSC model of the BC molecules. This result is consistent with the observation of not finding any tilted smectic phase in the earlier Monte Carlo simulation study using the HSC model of the BC molecules [26]. The bead model displays different behavior compared to the HSC model as shown in Fig. 7(b). For the bead model, the minimum of V_{ex} with respect to θ strongly depends on the bending angle of the molecules. The excluded volume V_{ex} is minimum at $\theta = 0^\circ$ for $\beta \leq 120^\circ$ and the minimum shifts to non zero value of θ for the higher bending angle. So, the SmAP layer is always stable compared to the SmCP layer order for bending angle $\beta \leq 120^\circ$. Whereas the excluded volume interaction favours the spontaneous tilt of the molecules in the layer for β greater than 120° giving rise to the chiral C_2 symmetry. This can perhaps explain the observation of tilted chiral crystal phases in the simulation results of BC molecules with $\beta = 140^\circ$ in the article [24]. Our result also agrees well with the molecular dynamics simulation studies of BC molecules with $\beta > 130^\circ$ [11].

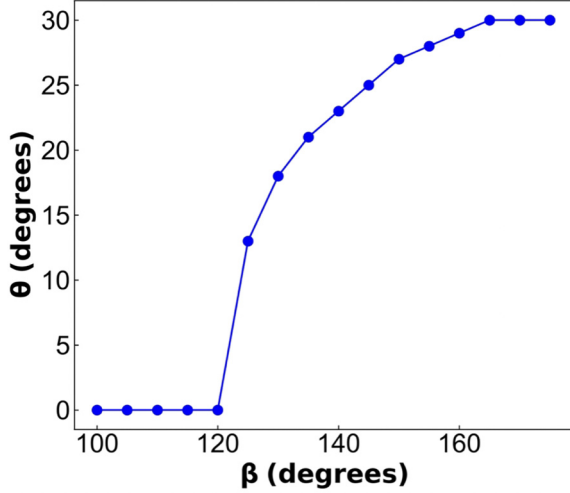


FIG. 8. The favoured tilt angle θ for the bead model of the BC molecules at different values of bending angle β .

Figure 8 depicts the variation of the favoured tilt angle as a function of the bending angle obtained from the excluded volume interaction. This tilt angle increases from zero beyond $\beta = 120^\circ$ and saturates to a value of 30° for nearly rodlike molecules with $\beta \sim 180^\circ$. This tilting of the molecules in the layer arises due to the close packing arrangements of the beads in the rodlike molecules. Similar tilt angles were also found in earlier simulation studies of BC molecules using the bead model with the Lennard-Jones interaction potential between the molecules [27]. The favored tilt angle is obtained on minimization of the excluded volume between two molecules in a layer and it can be called the effective optimal molecular tilt for each pair of molecules [33]. However, the average tilt of molecules in a layer in their smectic phase can be obtained by statistical averaging with this excluded volume interaction.

IV. MONTE CARLO SIMULATION

Excluded volume effects discussed above clearly favour the chiral tilted polar smectic phase with C_2 point symmetry of the layers for both the bead and HSC model of the BC molecules. However, excluded volume effects describe the properties of an athermal system. We have therefore constructed a coupled XY -Ising model to describe the cooperative development of chiral order in a layer as a function of temperature and electric field. Similar types of XY -Ising models have been employed over the past to describe superconducting Josephson-junction arrays in a transverse magnetic field [34,35]. These models have also been used to describe the ordered and disordered hexagonal columnar phases of discotic liquid crystals [36,37]. To the best of our knowledge, there is no report of the coupled XY -Ising model describing the phase transition in bent-core liquid crystals.

In this model, we assume that the BC molecules in a layer are tilted with respect to the layer normal with a fixed tilt angle but with variable tilt directions. Hence, the tilt direction of each molecule can be specified by a unit vector $\hat{\xi}$ as shown in Fig. 1. The tilt direction $\hat{\xi}$ lies on the layer plane and can be considered as an XY spin. Armed with our excluded volume

results, we assume that the roll angle ψ of a molecule can randomly take a value of either 0 or π . Thus the bending direction \hat{p} of a BC molecule can be parallel or antiparallel to the tilt direction $\hat{\xi}$ giving $\hat{p} = \sigma \hat{\xi}$ where σ is an Ising spin variable taking value ± 1 . Therefore, the Ising variable σ represents the chirality in the orientation of a BC molecule with respect to the layer.

We consider the orientational interaction potential between the molecules in a layer as $U_{ij} = -Jk_B(1 + A\sigma_i\sigma_j)(\hat{\xi}_i \cdot \hat{\xi}_j)$, where i, j denote the molecular indices and k_B is the Boltzmann constant. The first term favors a synclinic interaction between the molecules for the parameter $J > 0$ which has the dimension of temperature. We assume that this term gives the more dominant interaction between the molecules. The second term with the dimensionless coefficient A takes into account the synclinic homochiral or anticlinic recimic orientations between the molecules. From the geometry of the BC molecules, this term is expected to be lesser than the first term, i.e., $A < 1$. The potential due to an externally applied electric field is assumed as $U_i(\vec{E}) = -Jk_B\sigma_i\hat{\xi}_i \cdot \vec{E}$, where \vec{E} represents the effective electric field. Hence, the Hamiltonian of the system is defined as $H = \sum_{\langle i, j \rangle} U_{ij} + \sum_i U_i$, where $\langle \rangle$ denotes the sum over the nearest neighbor pairs of molecules.

We carried out Monte Carlo simulations on a square lattice of dimension 40×40 with periodic boundary conditions. The XY and Ising variables are updated by the standard Metropolis algorithm. One of the following three update schemes is chosen randomly: (i) selection of a new random direction for the XY variable $\hat{\xi}$ without flipping the Ising spin σ , (ii) flipping of σ with unaffected $\hat{\xi}$, and (iii) selection of a new random direction for $\hat{\xi}$ and flipping of σ . Similar update schemes were also used in MC simulation for the kinetics study of the coupled XY -Ising model [38]. For simulation at each temperature or electric field, 10^6 MC cycles were run for equilibration and additional 10^6 MC steps were performed to compute the statistical quantities. The tilt, polar, and chiral order parameters are defined as

$$\xi = \frac{1}{L^2} \left\langle \left| \sum_i^{L \times L} \hat{\xi}_i \right| \right\rangle,$$

$$P = \frac{1}{L^2} \left\langle \left| \sum_i^{L \times L} \hat{p}_i \right| \right\rangle, \text{ and } \sigma = \frac{1}{L^2} \left\langle \left| \sum_i^{L \times L} \sigma_i \right| \right\rangle,$$

respectively, where $\langle \rangle$ denotes the ensemble average and the sum runs over the total number of lattice points. The expression $C = \frac{\langle H^2 \rangle - \langle H \rangle^2}{L^2 k_B^2 T^2}$ was used for the calculation of the dimensionless specific heat per molecule where T is the absolute temperature. To study the equilibrium phases as a function of temperature, the simulation was started at a high temperature with an initial isotropic configuration. The initial temperature was chosen such that the system remains in its equilibrium isotropic state. In this isotropic configuration, each molecule is tilted in the layer but their tilt and polar directions are randomly oriented as shown in the leftmost configuration in Fig. 9. This configuration represents an achiral uniaxial smectic layer with no polar order. Therefore, the long axes of the molecules are distributed on the surface of a cone giving rise to the de Vries SmA layer structure with the

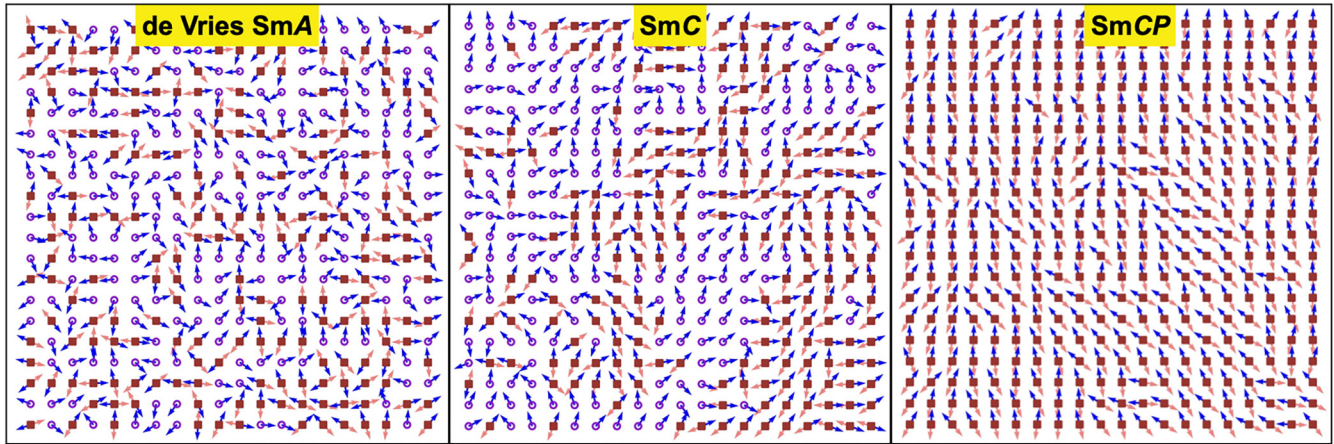


FIG. 9. The representative spin configurations corresponding to the different phases. The blue and red (light gray) arrows denote the orientations of the unit vectors $\hat{\xi}$ and $\hat{\rho}$, respectively. The open circle and filled square symbols represent +1 and -1 values of the Ising spin, respectively.

proposed diffused cone model [39]. The system was equilibrated at each temperature and the stable phase sequence was determined with decreasing temperature. The final equilibrated state of the system at a given temperature was chosen as the initial configuration for the MC simulation at the next lower temperature. The same procedure was adopted for studying the equilibrium phase sequence with increasing electric field. The equilibrium values of the order parameters as a function of temperature are shown in Fig. 10 for the model parameter $A = 0.5$. The tilt order parameter ξ of the system increases significantly from zero with decreasing temperature below about $T/J \sim 1.25$ while the other order parameters P and σ remain zero till about $T/J \sim 1.0$. Therefore, the system in this temperature range exhibits the nonpolar SmC structure. A typical configuration of the spins in the SmC structure is shown in Fig. 9. A small peak in the specific heat corresponds to this transition is also shown in the inset of Fig. 10. However, the ordering of the XY spins is expected to be quasiling range

in two dimensions according to Mermin-Wagner theorem [40] and the transition is of Kosterlitz-Thouless type [41]. Finite-size scaling analysis is required to accurately determine the transition temperature. On further cooling below about $T/J \sim 1.0$, the order parameters P and σ also become nonzero giving rise to a chiral tilted polar SmCP structure. A representative spin configuration in the SmCP structure is shown in Fig. 9. The larger peak in the specific heat as shown in the inset of Fig. 10 indicates this transition. Similar transitions are also speculated in the earlier studies on superconducting systems [34,35]. The chiral order parameter σ reaches the saturation value rapidly compared to the other order parameters across this transition. This is perhaps due to two possible states for the Ising spin compared to the continuum of states for the XY spin. The number of states of a spin variable increases the disorderedness in the system and it is reflected in the variation of order parameters with temperature. This type of phase sequence has been observed experimentally in bent-core liquid crystals [42]. Figure 11 displays the variation of order parameters with the electric field at a fixed temperature

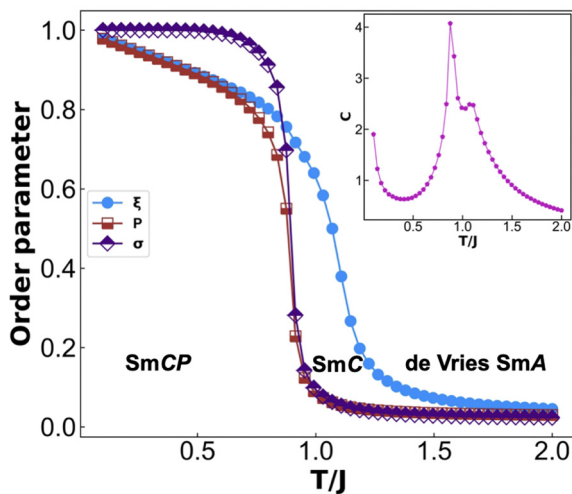


FIG. 10. The variation of order parameters with temperature for $A = 0.5$ at zero electric field. Inset shows the corresponding specific heat variation.

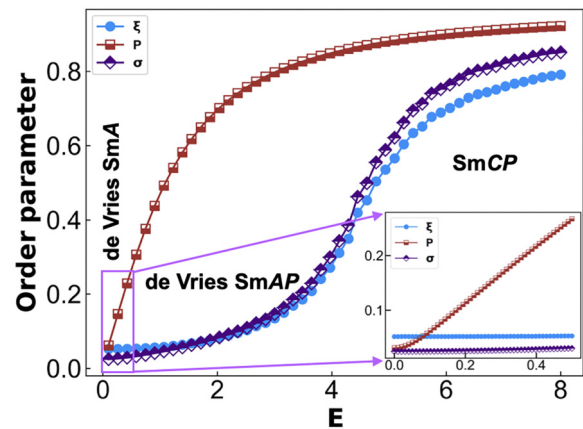


FIG. 11. The variation of order parameters with electric field for $T/J = 1.8$ and $A = 0.5$. Inset shows the magnified view of the region at low field.

TABLE I. The observed phase sequences for different values of A .

A	Phase sequences during cooling
0.0	de Vries SmA ($\{\xi, P, \sigma\} = 0$) \rightarrow SmC ($\{P, \sigma\} = 0, \xi \neq 0$)
0.5	de Vries SmA ($\{\xi, P, \sigma\} = 0$) \rightarrow SmC ($\{P, \sigma\} = 0, \xi \neq 0$) \rightarrow SmCP ($\{\xi, P, \sigma\} \neq 0$)
1.0	de Vries SmA ($\{\xi, P, \sigma\} = 0$) \rightarrow SmCP ($\{\xi, P, \sigma\} \neq 0$)

$T/J = 1.8$ corresponding to the de Vries SmA state. All the order parameters are zero at the low field region as expected in the de Vries SmA layer structure. Above a certain threshold field, the polar order P in the layer increases monotonically with the electric field whereas the other order parameters ξ and σ remain close to zero. Hence, the layer goes into the de Vries SmAP phase. In this phase, the bending direction \hat{p} of the molecules align on average along the field but the tilt direction $\hat{\xi}$ is equally likely oriented parallel or antiparallel to \hat{p} . Thus the long axes of the tilted molecules have a bimodal distribution around the diffused cone giving rise to an achiral biaxial polar layer structure. Above a higher threshold field, all the order parameters become nonzero and the chiral SmCP layer structure is stabilized. Therefore the layer exhibits spontaneous breaking of chiral symmetry. The electric field-induced breaking of chiral symmetry in bent-core liquid crystals has been reported [43].

The possible sequences of phases for different values of the model parameter A are given in Table I. For $A = 0$, there is no chiral or polar interaction between the molecules and only de Vries SmA and achiral SmC structures can be stabilized. For intermediate values of A , the de Vries SmA, SmC, and chiral SmCP structures are stable as discussed above. The tilt and polar interactions being comparable for $A = 1$, the de Vries SmA directly going to the chiral SmCP structure is favored. Therefore, achiral uniaxial nonpolar (de Vries

SmA), achiral biaxial nonpolar (SmC), achiral biaxial polar (de Vries SmAP), and chiral biaxial polar (SmCP) structures can be stabilized in our model depending on the parameter A , temperature and electric field. Analogous polar biaxial, nonpolar biaxial, and uniaxial phases have been found for nontilted bent-core molecules in a layer using molecular statistical theory with a different type of interaction potential [44]. All the results discussed above are obtained for a single layer in the smectic phase. In actual three-dimensional smectic liquid crystals, the interlayer interactions also play a significant role in the phase behavior and can lead to rich varieties of self-assembled structures (see for example [45]). It is therefore worthwhile to include these interlayer interactions along with the intralayer interactions in the simulation. We intend to study this model in three dimensions in the future.

V. CONCLUSIONS

We have computed the excluded volume between bent-core molecules in a layer of their smectic phases. Two molecular models namely the spherocylinder and bead model of the bent-core molecules were used in the computation of the excluded volume. The excluded volume results for both models of the BC molecules predict chiral symmetry breaking in their tilted smectic phase. This is the first report on the numerical studies of excluded volume between BC banana-shaped molecules in a layer of their smectic phase which accounts for the experimentally observed chiral symmetry breaking. Depending on the tilt and bending angle of the molecules, the bead model predicts the possibility of C_2 , C_s , and C_1 point symmetries of the layers. We have also developed a coupled XY-Ising model based on the excluded volume results to investigate the layer structure using Monte Carlo simulations as a function of temperature and electric field. The model predicts different types of phase sequences depending on the interaction parameter and also accounts for electric field-induced chiral symmetry breaking.

- [1] P. G. de Gennes and J. Prost, *The Physics of Liquid Crystals* (Clarendon Press, Oxford, 1995).
- [2] V. Borshch, Y. -K. Kim, J. Xiang, M. Gao, A. Jákli, V. P. Panov, J. K. Vij, C. T. Imrie, M. G. Tamba, G. H. Mehl, and O. D. Lavrentovich, *Nat. Commun.* **4**, 2635 (2013).
- [3] H. Takezoe and Y. Takanishi, *Jpn. J. Appl. Phys.* **45**, 597 (2006).
- [4] R. A. Reddy and C. Tschierske, *J. Mater. Chem.* **16**, 907 (2006).
- [5] A. Eremin and A. Jákli, *Soft Matter* **9**, 615 (2013).
- [6] T. Niori, T. Sekine, J. Watanabe, T. Furukawa, and H. Takezoe, *J. Mater. Chem.* **6**, 1231 (1996).
- [7] D. R. Link, G. Natale, R. Shao, J. E. Maclennan, N. A. Clark, E. Körblova, and D. M. Walba, *Science* **278**, 1924 (1997).
- [8] G. Heppke and D. Moro, *Science* **279**, 1872 (1998).
- [9] D. M. Walba, E. Körblova, R. Shao, J. E. Maclennan, D. R. Link, M. A. Glaser, and N. A. Clark, *Science* **288**, 2181 (2000).
- [10] S. Rauch, P. Bault, H. Sawade, G. Heppke, G. G. Nair, and A. Jákli, *Phys. Rev. E* **66**, 021706 (2002).
- [11] Y. Yang, H. Pei, G. Chen, K. T. Webb, L. J. Martinez-Miranda, I. K. Lloyd, Z. Lu, K. Liu, and Z. Nie, *Sci. Adv.* **4**, eaas8829 (2018).
- [12] Brand, H. R., Cladis, P. E., and Pleiner, H., *Eur. Phys. J. B* **6**, 347 (1998).
- [13] A. Jákli, D. Krüerke, H. Sawade, and G. Heppke, *Phys. Rev. Lett.* **86**, 5715 (2001).
- [14] N. Chattham, E. Korblova, R. Shao, D. M. Walba, J. E. Maclennan, and N. A. Clark, *Liq. Cryst.* **36**, 1309 (2009).
- [15] N. Chattham, E. Korblova, R. Shao, D. M. Walba, J. E. Maclennan, and N. A. Clark, *Phys. Rev. Lett.* **104**, 067801 (2010).
- [16] J. P. Bedel, J. C. Rouillon, J. P. Marcerou, H. T. Nguyen, and M. F. Achard, *Phys. Rev. E* **69**, 061702 (2004).
- [17] E. Gorecka, D. Pocięcha, N. Vaupotič, M. Čepič, K. Gomola, and J. Mieczkowski, *J. Mater. Chem.* **18**, 3044 (2008).
- [18] A. Eremin, S. Diele, G. Pelzl, H. Nádasi, and W. Weissflog, *Phys. Rev. E* **67**, 021702 (2003).

- [19] C. Bailey and A. Jákli, *Phys. Rev. Lett.* **99**, 207801 (2007).
- [20] C. Zhang, N. Diorio, S. Radhika, B. Sadashiva, S. N. Sprunt, and A. Jákli, *Liq. Cryst.* **39**, 1149 (2012).
- [21] N. Chattham, M.-G. Tamba, R. Stannarius, E. Westphal, H. Gallardo, M. Prehm, C. Tschierske, H. Takezoe, and A. Eremin, *Phys. Rev. E* **91**, 030502(R) (2015).
- [22] A. Roy, N. V. Madhusudana, P. Tolédano, and A. M. Figueiredo Neto, *Phys. Rev. Lett.* **82**, 1466 (1999).
- [23] P. J. Camp, M. P. Allen, and A. J. Masters, *J. Chem. Phys.* **111**, 9871 (1999).
- [24] J. Xu, R. L. B. Selinger, J. V. Selinger, and R. Shashidhar, *J. Chem. Phys.* **115**, 4333 (2001).
- [25] R. Memmer, *Liq. Cryst.* **29**, 483 (2002).
- [26] Y. Lansac, P. K. Maiti, N. A. Clark, and M. A. Glaser, *Phys. Rev. E* **67**, 011703 (2003).
- [27] A. Dewar and P. J. Camp, *Phys. Rev. E* **70**, 011704 (2004).
- [28] A. V. Emelyanenko and M. A. Osipov, *Phys. Rev. E* **70**, 021704 (2004).
- [29] L. Onsager, *Ann. NY Acad. Sci.* **51**, 627 (1949).
- [30] H. Goldstein, C. Poole, and J. Safko, *Classical Mechanics* (Addison-Wesley, Boston, 2001).
- [31] C. Vega and S. Lago, *Comput. Chem.* **18**, 55 (1994).
- [32] V. J. Lumelsky, *Information Processing Letters* **21**, 55 (1985).
- [33] A. V. Emelyanenko and A. R. Khokhlov, *J. Chem. Phys.* **142**, 204905 (2015).
- [34] E. Granato, J. M. Kosterlitz, J. Lee, and M. P. Nightingale, *Phys. Rev. Lett.* **66**, 1090 (1991).
- [35] J. Lee, E. Granato, and J. M. Kosterlitz, *Phys. Rev. B* **44**, 4819 (1991).
- [36] M. Hébert and A. Caillé, *Phys. Rev. E* **51**, R1651 (1995).
- [37] M. Hébert and M. L. Plumer, *Phys. Rev. E* **54**, 550 (1996).
- [38] J.-R. Lee, S. J. Lee, B. Kim, and I. Chang, *Phys. Rev. E* **54**, 3257 (1996).
- [39] A. de Vries, *J. Chem. Phys.* **71**, 25 (1979).
- [40] N. D. Mermin and H. Wagner, *Phys. Rev. Lett.* **17**, 1133 (1966).
- [41] J. M. Kosterlitz, *J. Phys. C* **7**, 1046 (1974).
- [42] A. Eremin, H. Nádasi, G. Pelzl, S. Diele, H. Kresse, W. Weissflog, and S. Grande, *Phys. Chem. Chem. Phys.* **6**, 1290 (2004).
- [43] A. A. S. Green, M. R. Tuchband, R. Shao, Y. Shen, R. Visvanathan, A. E. Duncan, A. Lehmann, C. Tschierske, E. D. Carlson, E. Guzman *et al.*, *Phys. Rev. Lett.* **122**, 107801 (2019).
- [44] M. S. Romashin and A. V. Emelyanenko, *Moscow Univ. Phys.* **68**, 249 (2013).
- [45] A. V. Emelyanenko, A. Fukuda, and J. K. Vij, *Phys. Rev. E* **74**, 011705 (2006).